3-Hydroxyanthranilic acid inhibits PDK1 activation and suppresses experimental asthma by inducing T cell apoptosis

Tomoko Hayashi*, Ji-Hun Mo*†, Xing Gong*, Cyprian Rossetto*, Angela Jang*, Lucinda Beck*, Gregory I. Elliott‡, Irina Kufareva§, Ruben Abagyan§, David H. Broide*, Jongdae Lee*, and Eyal Raz*¶

*Department of Medicine, University of California at San Diego, La Jolla, CA 92093-0663; ‡Moores Cancer Center, University of California at San Diego, La Jolla, CA 92093-0820; and §The Scripps Research Institute, La Jolla, CA 92037

Communicated by Dennis A. Carson, University of California at San Diego School of Medicine, La Jolla, CA, October 1, 2007 (received for review July 23, 2007)

3-Hydroxyanthranilic acid (HAA), a compound generated during tryptophan metabolism initiated by indoleamine 2,3-dioxygenase, is known to induce T cell death, but its molecular target is not known. Here we report that HAA inhibits NF-κB activation upon T cell antigen receptor engagement by specifically targeting PDK1. Inhibition of NF-κB by HAA leads to dysfunction and cell death of activated Th2 cells, which in turn suppresses experimental asthma. Inhibition of NF-κB and induction of apoptosis is specific to CD4 T cells because HAA does not inhibit NF-κB activation or induce cell death upon Toll-like receptor 4 stimulation in dendritic cells. Thus, HAA is a natural inhibitor that restrains T cell expansion and activation.

HAA | indoleamine 2,3-dioxygenase | NF-κB | tryptophan

Indoleamine 2,3-dioxygenase (IDO), the rate-limiting enzyme in tryptophan (trp) catabolism, is induced in various tissues mainly by IFN-γ (1, 2). IDO converts trp into *N*-formylkynurenine, which is further catabolized to kynurenine, 3-hydroxykynurenine, 3-hydroxyanthranilic acid (HAA), and the terminal metabolites quinolinic acid (QA) and picolinic acid (3) [supporting information (SI) Fig. 6]. The immunomodulatory function of IDO was first identified in the placenta, where it inhibits the rejection of fetal allografts (2, 4). Subsequent studies documented that IDO inhibits T cell proliferation *in vitro* (4, 5), promotes the survival of allografts (6–8), and ameliorates both experimental autoimmune encephalomyelitis (9) and trinitrobenzenesulfonic acid-induced colitis (10).

Previous reports demonstrated that the depletion of trp by IDO in the intracellular pool or microenvironment mediated an antimicrobial activity (11). Similar logic was applied to explain the immunomodulatory effects induced by IDO (4, 5, 12, 13). In contrast to these earlier reports, recent evidence has suggested that the intermediates of trp metabolism mediate the diverse immunomodulatory effects on T cells and monocyte-derived cells (14–18). HAA was shown to cause apoptosis in Th1 cells by caspase-8 activation (15), but its primary molecular target is yet unknown.

Experimental asthma is characterized by airway hyperresponsiveness (AHR) and lung inflammation provoked by allergen-specific Th2 lymphocytes. We recently showed that the induction of IDO by certain Toll-like receptor ligands suppresses experimental asthma by the induction of Th2 lymphocytes apoptosis (19). In this study, we explored the potential role of HAA, a trp metabolite, in the inhibition of experimental asthma, and we investigated the molecular pathway by which HAA regulates T cell functionality and survival. Our data demonstrate that HAA suppresses T cell antigen receptor (TCR)-triggered NF-κB activation by directly inhibiting PDK1 phosphorylation.

Results

HAA Inhibits NF-κB Activation upon TCR Engagement. To elucidate how HAA inhibits CD4 T cell activity, TCR signal-transduction pathways were analyzed after costimulation with anti-CD3/CD28 mAbs. HAA specifically inhibited the activation of NF-κB, but not JNK, ERK, or NFAT in ovalbumin (OVA)-specific *in vitro* differentiated tgTh2 cells (derived from DO11.10) (Fig. 1*A*). This observation was reproduced in Jurkat cells (a human CD4 T cell line) (Fig. 1*B*). However, HAA did not affect LPS-induced NF-κB activation in RAW264.7 cells and in bone marrow-derived dendritic cells (BMDC) or cytokine production (IL-6 and IL-12) in BMDC (SI Fig. 7 *A* and *B*).

The detailed mechanism of HAA-mediated inhibition of NF-κB activation was further investigated in Jurkat cells. HAA inhibited TCR-induced IκB kinase (IKK) activity, resulting in an impaired degradation of IκBα (Fig. 1*C*). To evaluate whether IKK is the direct target of HAA, IKK immunoprecipitates from unstimulated Jurkat cells were incubated with different concentrations of HAA or a known IKK inhibitor, BMS-345541 (BMS) (20); IKK activity was measured by an *in vitro* kinase assay. Although BMS inhibited IKK activity as expected, HAA did not (Fig. 1*D*), indicating that IKK is not a direct target of HAA. The signaling molecules upstream to IKK in the TCR activation pathways were then examined. As presented in Fig. 1*E*, HAA did not inhibit the activation of PLCγ1, an upstream molecule of NFAT and ERK, or PKCθ, an upstream molecule of NF-κB (see also TCR signaling pathways in SI Fig. 8).

Because overexpression of certain upstream signaling molecules of NF-κB induces its activation (21), we used an NF-κB reporter assay in HEK-293 cells to identify the molecular target of HAA inhibition in TCR signaling pathways. NF-κB activation induced by PKCθ A/E (22), Carma1, or Bcl10 overexpression was not affected by HAA (SI Figs. 8 and 9).

HAA Inhibits PDK1. Although signals from both TCR (CD3) and CD28 are needed for complete activation of NF-κB (23), stimulation of CD28 alone is sufficient to induce a weak IKK activation (24). HAA inhibited NF-κB activation triggered by either CD28 alone or CD3/CD28 costimulation (Fig. 2*A*). Be-

Author contributions: T.H. and J.-H.M. contributed equally to this work; T.H., J.-H.M., J.L., and E.R. designed research; T.H., J.-H.M., X.G., C.R., A.J., L.B., and G.I.E. performed research; I.K., R.A., and D.H.B. contributed new reagents/analytic tools; T.H., J.-H.M., and E.R. analyzed data; and T.H., J.-H.M., and E.R. wrote the paper.

The authors declare no conflict of interest.

Abbreviations: AHR, airway hyperresponsiveness; BALF, bronchial alveolar lavage fluid; BMDC, bone marrow-derived dendritic cells; BMS, BMS-345541; HAA, 3-hydroxyanthranilic acid; IDO, indoleamine 2,3-dioxygenase; IKK, IκB kinase; i.n., intranasally; OVA, ovalbumin; QA, quinolinic acid; TCR, T cell antigen receptor; trp, tryptophan.

†Present address: Department of Otorhinolaryngology, Seoul National University, Bundang Hospital, Seongnam-Si, Korea 463-707.

¶To whom correspondence should be addressed. E-mail: eraz@ucsd.edu.

This article contains supporting information online at www.pnas.org/cgi/content/full/0709261104/DC1.

© 2007 by The National Academy of Sciences of the USA

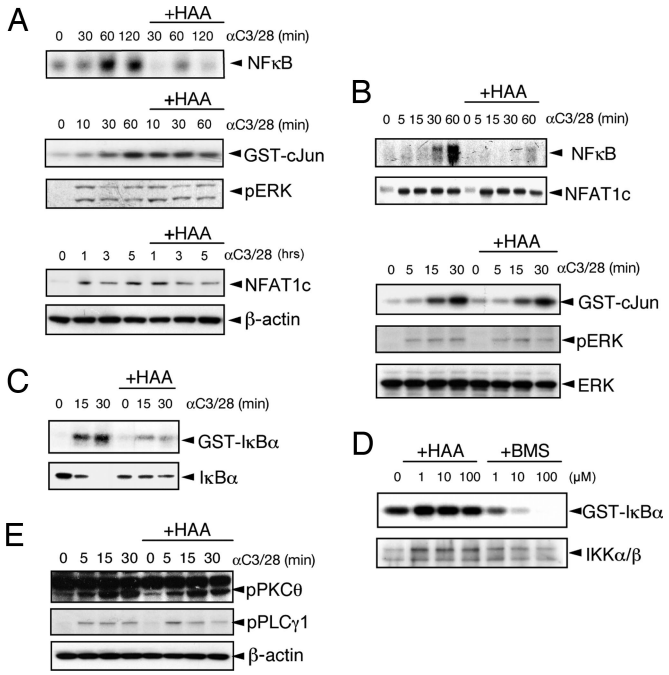

Fig. 1. HAA inhibits TCR-mediated NF-κB activation. (*A*) HAA inhibits NF-κB activation in tgTh2 cells. Th2 cells were stimulated with anti-CD3/CD28 mAbs with or without 100 μM HAA as indicated. NF-κB activity was measured by EMSA, and JNK was measured by an *in vitro* kinase assay. Cytosolic lysates were used for immunoblotting with anti-pERK and anti-NFAT1c Abs. (*B*) HAA inhibits NF-κB activation in Jurkat cells. Jurkat cells were stimulated with anti-CD3/CD28 mAbs with or without 100 μM HAA. NF-κB and NFAT, JNK, and ERK were detected as before. (*C*) TCR-mediated IKK activity and IκBα degradation are impaired in HAA-pretreated Jurkat cells. IKK activity was evaluated by an *in vitro* kinase assay, and IκBα and IKKα/β were detected by immunoblotting. (*D*) HAA does not directly inhibit IKK. Immunoprecipitates from unstimulated Jurkat cell lysates were incubated with different concentrations of HAA or BMS for 30 min, and IKK activity was measured by an *in vitro* kinase assay. (*E*) HAA does not alter TCR-induced activation of PLCγ1 and PKCθ. Cytosolic lysates were immunoblotted with anti-pPLCγ1 and anti-pPKCθ Abs.

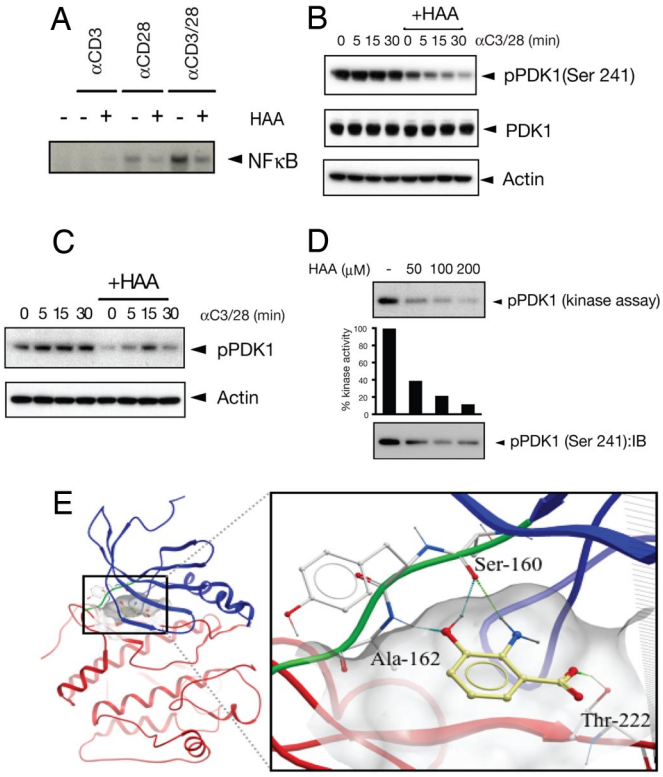

Fig. 2. HAA inhibits phosphorylation of PDK1. (*A*) HAA inhibits NF-κB activation upon anti-CD28 stimulation in Jurkat cells. Jurkat cells were preincubated with or without 100 μM HAA for 30 min and stimulated with anti-CD3, anti-CD28, or anti-CD3/CD28 mAbs for 30 min. NF-κB activity was measured by EMSA. (*B* and *C*) Cytosolic lysates were used for immunoblotting with anti-pPDK1 and anti-PDK1 Abs in Jurkat cells (*B*) and tgTh2 cells (*C*). (*D*) HAA inhibits PDK1 kinase activity in a dose-dependent manner. (*Top*) Recombinant PDK1 was incubated with different concentrations of HAA, and an *in vitro* kinase assay was performed to measure autophosphorylation of PDK1. (*Middle*) Its relative intensity is compared with control. (*Bottom*) Ser-241 phosphorylation of PDK1 was measured by immunoblotting. (*E*) Virtual docking of HAA to PDK1 by using ICM molecular software. (*Left*) An overall view of the PDK1 with HAA in the best scoring conformation. The N-terminal lobe is colored blue, the C-terminal lobe is red, and the hinge region is green. The surface of the active site is shown as transparent gray skin. (*Right*) A close-up view of the HAA molecule docked into the active site of PDK1. The molecule makes hydrogen bonds (shown in dots) with the backbone atoms of the hinge region (Ser-160 and Ala-162), as do most kinase inhibitors. Additionally, HAA makes a hydrogen bond with the side-chain oxygen of Thr-222. The top portions of the protein and pocket skin are clipped for clarity.

cause PDK1 is an essential mediator of CD28-induced NF-κB activation (23), we next tested whether PDK1 activity is affected by HAA. PDK1 is activated constitutively in Jurkat cells (25) (Fig. 2*B*), and HAA suppressed its phosphorylation at the Ser-241 site (Fig. 2*B*), which is essential for PDK1 activity (26). This inhibition was reproduced in tgTh2 cells (Fig. 2*C*). Because PDK1 autophosphorylates this site (27–29), we hypothesized that HAA either inhibits PDK1 directly or activates a phosphatase that dephosphorylates PDK1. To test the former possibility, we performed a PDK1 *in vitro* kinase assay. Recombinant PDK1 was incubated with different doses of HAA, and autophosphorylation of PDK1 was measured. HAA inhibited autophosphorylation of PDK1 at the Ser-241 site in a dose-dependent manner (Fig. 2*D*). To gain further insight into the structural basis of this inhibition of PDK1 phosphorylation by HAA, we used the flexible ligand-docking module of ICM molecular software (30). The predicted mode of interaction suggested that HAA binds in the ATP-binding site and makes direct hydrogen bonds with the backbone atoms of the hinge region (Ser-160 and Ala-162), as well as an additional hydrogen bond with the side-chain oxygen of Thr-222 (Fig. 2*E*). Taken together these data indicate that HAA inhibits NF-κB activation upon TCR engagement by inhibiting PDK1 phosphorylation (see also TCR signaling pathways in SI Fig. 8).

HAA Inhibits T Cell Activation and Induces T Cell Death at Different Concentrations. Activation of NF-κB regulates lymphocyte activation and survival. In a dose-dependent manner, HAA inhibited tgTh1 cytokine secretion (Fig. 3*A*) and provoked tgTh1 cell death (Fig. 3*B*). Similarly, HAA inhibited cytokine secretion (Fig. 3*C*) and proliferation (Fig. 3*D*) of tgTh2 cells and enhanced tgTh2 cell apoptosis (Fig. 3*E*). However, at a lower concentration (50 μM), HAA inhibited tgTh2 functionality without inducing T cell death (Fig. 3 *C* and *D* vs. *E*). Elevated caspase activities (CaspaTag) determined by FACS suggested that HAA provokes apoptosis of these cells (data not shown). Quinolinic acid (QA) (see SI Fig. 6), another trp metabolite that did not inhibit TCR-mediated NF-κB activation (data not shown), did not inhibit cytokine secretion or induce cell death in tgTh1 and tgTh2 cells (Fig. 3). HAA also induced cell death in Jurkat cells (data not shown).

However, consistent with the observation that HAA did not affect LPS-induced NF-κB activation (SI Fig. 7*A*), induction of cytokines (SI Fig. 7*B*), or induction of costimulatory molecules (SI Fig. 7 *C* and *D*), it also did not provoke cell death in LPS-stimulated BMDC (SI Fig. 7*E*). An inhibitor of IKKβ

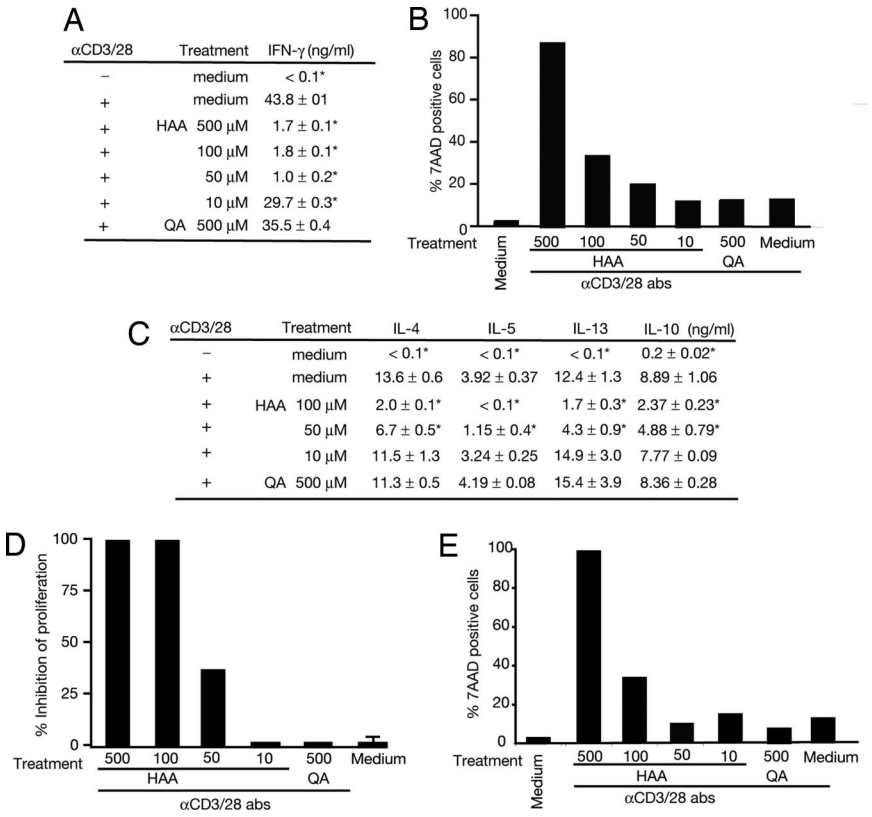

Fig. 3. HAA inhibits T cell function and induces apoptosis *in vitro*. (*A*) HAA inhibits IFN-γ production upon TCR engagement in Th1 cells. TgTh1 cells were activated with anti-CD3/CD28 mAbs for 48 h in the presence or absence of various concentrations of HAA or QA. *, $P < 0.05$, compared with control. (*B*) HAA induces apoptosis in activated Th1 cells. TgTh1 cells were activated with anti-CD3/CD28 mAbs for 48 h in the presence or absence of various concentrations of HAA or QA. The percentage of cell death was determined in the $CD4^+$/DO11.10 TCR^+ subset by staining with 7-AAD (FACS). (*C*) HAA inhibits cytokine production upon TCR engagement in Th2 cells. TgTh2 cells were activated with anti-CD3/CD28 mAbs for 48 h in the presence or absence of various concentrations of HAA or QA. *, $P < 0.05$, compared with control. (*D*) HAA inhibits proliferation of Th2 cells. After 48 h of incubation of tgTh2 cells with anti-CD3/CD28 mAbs in the absence or presence of HAA or QA, 1 μCi [^{3}H]thymidine was added, cells were further incubated for 24 h, and [^{3}H]thymidine incorporation was measured for cell proliferation. *, $P < 0.05$, compared with the cells stimulated with anti-CD3/CD28 Abs. (*E*) HAA induces apoptosis in activated Th2 cells. TgTh2 cells were activated with anti-CD3/CD28 Abs for 48 h in the presence or absence of various concentrations of HAA or QA. The percentage of cell death was determined in the $CD4^+$/DO11.10 TCR^+ subset by staining with 7-AAD (FACS).

(BMS) inhibited TCR-mediated NF-κB activation and induced cell death in tgTh2 cells (SI Fig. 10 *A–C*). Furthermore, a PDK1 inhibitor, KP372-1, also produced a similar result (SI Fig. 10 *D* and *E*). Collectively, these data support that HAA targets PDK1 and consequently inhibits NF-κB activation. The inhibition of this pathway of T cell activation is most likely responsible for the suppression of T cell functions at lower HAA concentrations and the induction of T cell death at higher HAA concentrations.

HAA Inhibits Th2-Induced Experimental Asthma. We next explored whether HAA-induced apoptosis can inhibit Th2-cell mediated inflammation *in vivo* by using a model of experimental asthma. OVA/alum-primed BALB/c mice were challenged with OVA and then treated with or without 100 μg of intratracheal HAA. HAA treatment suppressed AHR (measurement of % Penh) (Fig. 4*A*) and airway resistance (data not shown), compared with PBS (control) or QA treatment. Lower eosinophil counts were observed in the bronchoalveolar lavage fluid (BALF) of HAA-treated mice (Fig. 4*B*). The administration of HAA also reduced the levels of Th2 cytokines in the BALF (IL-5 and IL-13) (Fig. 4*B*). Histological examination revealed a lack of peribronchial and perivascular mononuclear cell infiltration and intact epithelial structure in the lungs of HAA-treated mice (Fig. 4*D*), compared with PBS-treated mice (Fig. 4*C*). In concentrations as low as 25 μg per animal, HAA significantly inhibited asthmatic parameters (Fig. 4*E*).

HAA Inhibits Th2 Cell Function and Induces Th2 Cell Death *in Vivo*. To confirm that the antiasthmatic effects of HAA are due to inactivation and/or induction of apoptosis in activated Th2 cells, we adoptively transferred *in vitro*-differentiated, OVA-specific tgTh2 cells into SCID mice. OVA-challenged recipients treated with HAA showed reduced levels of eosinophil and lower levels of Th2 cytokines in the BALF (Fig. 5*A*). The number of viable tgTh2 cells in the lungs of HAA-treated, OVA-challenged mice was significantly reduced (Fig. 5*B*), whereas the percentage of cell death of tgTh2 cells in HAA-treated, OVA-challenged mice was significantly increased, compared with those of PBS-treated, OVA-challenged animals (Fig. 5*C*). These results suggest that HAA suppresses experimental asthma by inhibiting Th2 cell function and inducing Th2 cell death.

Discussion

Although HAA is known to inhibit CD4 T cell functions, its molecular target has remained largely unknown. As presented earlier, HAA specifically inhibited TCR-induced NF-κB activation (Fig. 1 *A* and *B*). Although HAA inhibited IKK activity, the IKK complex was not directly affected by HAA (Fig. 1*C*). Strong activation of NF-κB by TCR signaling requires the triggering of both CD3 and CD28 (24), whereas stimulation of CD28 alone induces weak activation, prompting our investigation of transducers downstream to CD28. PDK1 is a key mediator of CD28-induced activation of NF-κB (SI Fig. 8). Phosphatidyli-

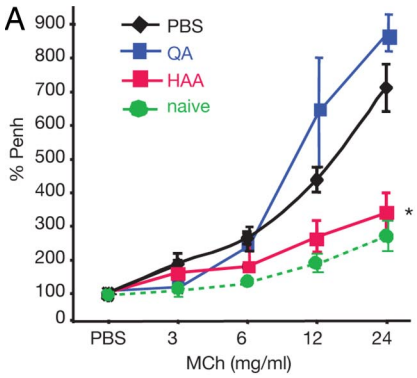

B

Treatment	Eo (x10^4)	(pg/ml) IL-5	IL-13
PBS	33.1 ± 5.2	398 ± 98	170 ± 53
HAA	15.5 ± 4*	141 ± 54*	66 ± 32*
QA	33.5 ± 6.6	312 ± 51	263 ± 64
naive	< 0.1*	< 15*	< 15*

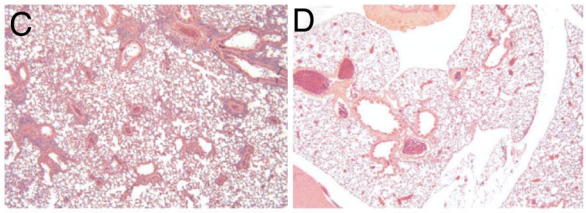

E

Treatment	PC200	BAL Eo (x10^4)	IL-5	IL-13 (pg/ml)
PBS	3.14 ± 0.56	28.7 ± 5.3	307 ± 57	143 ± 29
HAA 100 μg	8.8 ± 1.18*	8.4 ± 1.3*	153 ± 27*	88 ± 15*
HAA 25 μg	7.26 ± 1.16*	5.8 ± 4.3*	144 ± 26*	91 ± 18*
HAA 6 μg	3.82 ± 0.96	19 ± 7.5	219 ± 27	147 ± 39

Fig. 4. HAA inhibits experimental asthma. (*A*) HAA reduces allergic AHR in an experimental asthma model. BALB/c mice were immunized with OVA in alum s.c. on days 0 and 7, challenged with OVA i.n. on days 15 and 20, and treated with 100 μg of trp metabolites intratracheally 4 h after the OVA challenge. HAA-treated mice showed decreased AHR compared with PBS-treated mice. (*B*) HAA treatment reduces eosinophil (Eo) infiltration and Th2 cytokine levels in the BALF. The total cell number and the differential cell count in BALF were determined as described (19). (*C* and *D*) HAA reduces peribronchial and perivascular eosinophil infiltration (*C*, PBS-treated mice; *D*, HAA-treated mice) (H&E staining). (Magnification: ×40.) (*E*) In a dose-dependent manner, HAA inhibits asthmatic parameters. Data shown are means ± SEM of four to six mice per group of one of four independent experiments that yielded similar results. *, $P < 0.05$, compared with PBS-treated mice.

nositides serve as second messengers recruiting downstream effectors containing pleckstrin homology domains, such as PDK1 and PKB/Akt, to the plasma membranes (23), whereby PKB/Akt is then fully activated by PDK1 (31). HAA inhibited the phosphorylation of PDK1 at Ser-241, a site essential for PDK1 (Fig. 2 *B* and *C*) autophosphorylation (29, 32). Exploration of the mode of interaction between HAA and PDK1 by using computer modeling predicted the most plausible docking site for HAA on PDK1 to be around Ser-160 to Thr-222, and it suggested that HAA is likely to bind to PDK1 in that particular conformation, resulting in the inhibition of PDK1 autophosphorylation/activation.

In antigen-stimulated lymphocytes, NF-κB induces the expression of multiple genes necessary for survival, proliferation, and effector functions (33). We therefore evaluated the physiological implications of HAA inhibition of PDK1 phosphorylation and NF-κB activation upon CD3/CD28 stimulation. Under these conditions, blockade of NF-κB activation by HAA inhibits T cell functions at lower HAA concentrations and induces T cell death at higher HAA concentrations (Fig. 3). Other inhibitors of NF-κB activation, BMS and KP372-1 (by the inhibition of PDK1), also induced T cell death (SI Fig. 10). However, the inhibition of PDK1 activation can affect T cell survival independently of Akt phosphorylation. PDK1 deletion prevents the expression of key nutrient receptors in T cells, in particular CD71 (the transferrin receptor) and CD98 (a subunit of L-amino acid transporters) (34). The loss of nutrient receptors can compromise T cell proliferative response, upon TCR ligation, and consequently promotes T cell death. In marked contrast to its effects on T cells, HAA, at any concentration tested, did not affect BMDC survival or maturation upon LPS stimulation (SI Fig. 7).

Our investigation into whether HAA can suppress experimental asthma, a Th2 cell-mediated disease, revealed that the administration of HAA inhibited AHR, airway resistance, and allergic lung inflammation (Fig. 4). Although HAA inhibited Th2 cell function (Fig. 5*A*), induction of apoptosis by this compound was modest (Fig. 5*C*). In *in vitro* studies, HAA inhibited cytokine production and T cell proliferation at a lower concentration than that required to induce T cell death (Fig. 3 *C*–*E*). Thus, these *in vivo* data suggest that inhibition of Th2 cell activation also plays a role in suppressing this Th2-mediated lung inflammation.

Previous reports have demonstrated an inhibition of Th1-mediated responses by trp metabolites. A derivative of HAA, *N*-(3,4,-dimethoxycinnamoyl) anthranilic acid, was shown to inhibit Th1-mediated experimental autoimmune encephalomyelitis. Another study showed that inhibition of IDO aggravated Th1-mediated colitis (9, 10), and an *in vitro* study demonstrated a Th1 susceptibility to HAA (15). We demonstrated here that HAA inhibits CD4 cells (Th1, Th2, and Jurkat) regardless of their Th phenotype. Therefore, the potential immunomodulatory properties of HAA can be applied to the inhibition of Th1-, Th2-, and Th17-mediated inflammation.

A

Challenge	Treatment	Eo (x10^4)	IL-5	IL-13 (pg/ml)
PBS	PBS	< 0.1	< 10	< 10
OVA	PBS	2.8 ± 0.5*	106 ± 17*	150 ± 23*
OVA	HAA	1.1 ± 0.2**	< 10**	< 10**

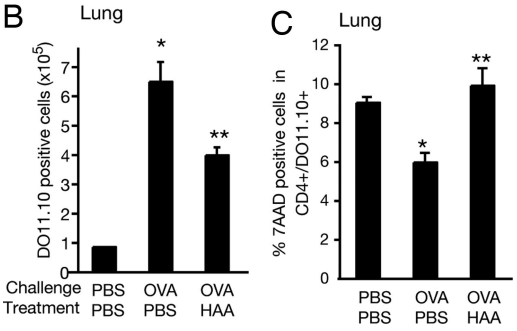

Fig. 5. HAA inhibits Th2 cell function and induces apoptosis of activated Th2 cells *in vivo*. OVA-specific tgTh2 cells (5×10^6 per mouse) were transferred to SCID mice i.v. on day 0. Mice were challenged i.n. with 50 μg of OVA on days 1 through day 4 and received 100 μg of HAA 4–6 h after the i.n. OVA challenge. Mice were evaluated on day 5. (*A*) HAA inhibits eosinophil (Eo) infiltration and Th2 cytokine production in the BALF. Data shown are means ± SEM of four mice per group from one of three independent experiments that yielded similar results. (*B*) HAA reduces the number of viable tgTh2 cells in the lungs. The total number of cells in the lung was calculated by multiplication of the total number of live cells by the percentage of CD4$^+$/DO11.10 TCR$^+$ cells in the cell suspension. (*C*) HAA increases the percentage of tgTh2 cell death in the lung. The percentage of tgTh2 cell death in lungs was determined by staining with 7-AAD (FACS) and analyzing T cells inside the CD4$^+$/DO11.10 TCR$^+$ gated population. *, $P < 0$, compared with PBS-challenged mice. **, $P < 0.05$, compared with OVA-challenged and PBS-treated mice.

Materials and Methods

Animals. WT BALB/c, transgenic (tg) DO11.10 mice (BALB/c) and SCID mice (BALB/c) were purchased from The Jackson Laboratory (Bar Harbor, ME) or Harlan (Indianapolis, IN). All animal procedures were performed following University of California at San Diego Animal Care guidelines.

Reagents. OVA, 3-HAA, QA, and KP372-1 were purchased from Sigma–Aldrich (St Louis, MO). Endotoxin levels in the reagents were measured by using the QCL1000 kit purchased from BioWhittaker (Walkerville, MD). Only reagents that contained <1 pg of endotoxin per 1 μg of reagent were used throughout the experiments. The IKK inhibitor, BMS [*N*1-(1,8-dimethylimidazo[1,2-a]quinolin-4-yl)-ethane-1,2-diamine], was prepared in seven steps according to the procedure described in the PCT patent application (WO 02/060386 A2), beginning with commercially available starting materials, 3-fluoro-4-nitrotoluene and ethyl 4-methyl-5-imidazole carboxylate. The compound was isolated and used as the HCl salt form.

Cell Culture and Abs. Complete media (RPMI medium1640; Irvine Scientific, Irvine, CA) supplemented with 10% heat-inactivated FCS, 2 mM L-glutamine, 100 units/ml penicillin, and 100 μg/ml streptomycin were used throughout the experiments. Jurkat cells were cultured in complete medium. HEK-293 cells were cultured in DMEM supplemented with 10% FCS and 2 mM L-glutamine. *In vitro*-differentiated tgTh1 or tgTh2 cells (10^6) (19) were incubated with or without plate-bound anti-CD3 mAb (BD PharMingen, San Diego, CA) and 1 mg/ml soluble anti-CD28 mAb (BD Pharmingen) in complete medium in the presence or absence of HAA or other compounds.

We used the following Abs: anti-pERK, anti-NFAT1c, anti-pPKCθ, anti-pPLCγ1, anti-PDK1, and anti-pPDK1 (Cell Signaling Technology, Danvers, MA); anti-IKK, anti-IκBa, anti-IκB, and anti-ERK (Santa Cruz Biotechnology, Santa Cruz, CA); and anti-β-actin (Sigma–Aldrich).

***In Vitro* Kinase Assays and EMSA.** Kinase assays and EMSA were performed as described (35). Briefly, for *in vitro* kinase assays, immunoprecipitated JNK1 or IKK were incubated with their respective recombinant substrate, GST-cJun or GST-IκBα, and [γ-^{32}P]ATP for 30 min. The reaction mixture was subjected to SDS/PAGE, followed by autoradiography. Translocation of activated NF-κB into the nucleus was measured by EMSA by using consensus NF-κB oligonucleotides (Santa Cruz Biotechnology) labeled with [γ-^{32}P]ATP. Activation of ERK, PLC-γ, PKC, and PDK1 was measured by Western blotting with respective anti-phospho Abs.

***In Vitro* PDK1 Kinase Assay.** For the *in vitro* PDK1 kinase assay, 60 ng of recombinant PDK1 (Upstate Biotechnology, Lake Placid, NY) was incubated with different concentrations of HAA without substrate for 30 min in kinase buffer (35), followed by 30 min incubation at 25°C after the addition of [γ-^{32}P]ATP. The reaction was then subjected to SDS/PAGE, followed by autoradiography. To verify the autophosphorylation site, the same sample was probed with anti-*p*-PDK1 (Ser-241) Ab (Cell Signaling Technology).

NF-κB Reporter Assay. HEK-293 cells grown in 12-well plates were transfected with the indicated plasmid together with NF-κB luciferase and β-gal constructs by using Lipofectamine 2000 (Invitrogen). The type and quantity of plasmids used were as follows: 50 ng of NF-κB luciferase, 10 ng of β-gal, 250 ng of PKCθ A/E (obtained from C. Elly, La Jolla Institute for Allergy and Immunology, San Diego, CA), 100 ng of Carma1 (obtained from M. Thorme, University of Lausanne, Lausanne, Switzerland), and 500 ng of Bcl10 (obtained from M. Thorme); 100 μM HAA was added 2 h after transfection. Twelve hours after transfection, cells were lysed, and luciferase activity was measured by using a luciferase assay kit (BD Biosciences). β-gal activity was measured to normalize the NF-κB activity by using the β-gal kit (Promega, Madison, WI).

Prediction of Molecular Interaction Between HAA and PDK1. The soft flexible docking unit of the ICM software (30) was used to simulate docking of HAA into the active sites of the available PDK1 structures. Among several plausible ligand poses/conformations, the one having the lowest ICM score was chosen. A low ICM score indicated that the ligand was likely to bind to PDK1 in this conformation.

Effects of HAA and Other Inhibitors on Cell Proliferation and Apoptosis. *In vitro*-differentiated tgTh1 or tgTh2 cells (10^6) were incubated for 48 h with plate-bound anti-CD3 mAb (BD Pharmingen) and 1 mg/ml soluble anti-CD28 mAb (BD Pharmingen) in the presence or absence of HAA, QA, or KP372-1 at the indicated concentrations. TgTh cells were stained for CD4 (BD Pharmingen) and DO11.10 TCR (Caltag, Burlingame, CA). Dead cells were stained with 7-AAD (BD Pharmingen) according to the manufacturer's instructions. Apoptotic cells were detected by a CaspaTag assay kit (Chemicon, Temecula, CA). BMDC were prepared from BALB/c as described (36). BMDC were treated with HAA in complete media up to 48 h with or without LPS stimulation. BMDC were stained for CD11c, CD80, CD86, and CD40. The stained cells were analyzed by using a FACSCalibur flow cytometer (Becton Dickinson, San Jose, CA). The levels of the various cytokines in the supernatants were determined by ELISA (BD Pharmingen).

For proliferation assay, 2×10^4 tgTh2 cells were preincubated with HAA, QA, or BMS for 30 min and then stimulated with

anti-CD3/CD28 mAbs for 48 h in 96-well plates. Then 1 μCi of [^{3}H]thymidine was added for another 24 h, and cell proliferation was assessed by measuring [^{3}H]thymidine incorporation.

Induction of Experimental Asthma. Induction of experimental asthma was performed as described (19). Briefly, mice were sensitized with 20 μg of OVA in 500 μg of alum by s.c. injection on days 0 and 7 and challenged intranasally (i.n.) with 20 μg of OVA on days 16 and 21. Four hours before the OVA challenge, mice received trp metabolites intratracheally as indicated. Twenty hours after the last challenge, airway responsiveness and airway resistance to methacholine were measured (19), followed by collection of BALF and harvesting of the lungs. The total number and the differential cell count in BALF were determined as described (19). The levels of IL-5 and IL-13 in the BALF were determined by ELISA (BD Pharmingen).

Adoptive Transfer. The adoptive transfer of 5×10^6 tgTh2 cells into SCID mice was performed as described (19), followed by i.n. sensitization with 50 μg of OVA daily for 4 days. Then 100 μg of HAA or PBS was given i.n. before each challenge. On day 5, mice were killed, and the BALF was collected to determine cytokine levels (ELISA). BALF cells were Wright–Geimsa stained (37). Single cell suspensions of lungs were prepared by collagenase digestion as described (38). Lung cells were stained for CD4 (BD Pharmingen), DO11.10 TCR (Caltag), and 7-AAD (BD Pharmingen) and analyzed by using a FACSCalibur flow cytometer (Becton Dickinson). The total cell number was calculated by multiplying the total number of live cells by the percentage of $CD4^+/DO11.10^+$ cells.

Statistical Analysis. Data are expressed as mean ± SEM. Data are compared by Student's *t* test. *P* values of <0.05 were considered significant.

We thank Jürg Tschopp (University of Lausanne, Lausanne, Switzerland), Margot Thome, and Chris Elly for their generous gift of plasmids. This work was supported by National Institutes of Health Grants AI57709, AI40682, HL79449, and DK35108.

1. Yoshida R, Urade Y, Tokuda M, Hayaishi O (1979) *Proc Natl Acad Sci USA* 76:4084–4086.
2. Munn DH, Zhou M, Attwood JT, Bondarev I, Conway SJ, Marshall B, Brown C, Mellor AL (1998) *Science* 281:1191–1193.
3. Moffett JR, Namboodiri MA (2003) *Immunol Cell Biol* 81:247–265.
4. Munn DH, Shafizadeh E, Attwood JT, Bondarev I, Pashine A, Mellor AL (1999) *J Exp Med* 189:1363–1372.
5. Hwu P, Du MX, Lapointe R, Do M, Taylor MW, Young HA (2000) *J Immunol* 164:3596–3599.
6. Grohmann U, Orabona C, Fallarino F, Vacca C, Calcinaro F, Falorni A, Candeloro P, Belladonna ML, Bianchi R, Fioretti MC, *et al.* (2002) *Nat Immunol* 3:1097–1101.
7. Sakurai K, Zou JP, Torres NI, Tschetter JR, Kim HS, Shearer GM (2002) *Transplant Proc* 34:3271–3273.
8. Swanson KA, Zheng Y, Heidler KM, Mizobuchi T, Wilkes DS (2003) *Am J Respir Cell Mol Biol* 30:311–318.
9. Sakurai K, Zou JP, Tschetter JR, Ward JM, Shearer GM (2002) *J Neuroimmunol* 129:186–196.
10. Gurtner GJ, Newberry RD, Schloemann SR, McDonald KG, Stenson WF (2003) *Gastroenterology* 125:1762–1773.
11. MacKenzie CR, Hadding U, Daubener W (1998) *J Infect Dis* 178:875–878.
12. Taylor MW, Feng GS (1991) *FASEB J* 5:2516–2522.
13. Kudo Y, Boyd CA, Sargent IL, Redman CW (2001) *J Physiol* 535:207–215.
14. Morita T, Saito K, Takemura M, Maekawa N, Fujigaki S, Fujii H, Wada H, Takeuchi S, Noma A, Seishima M (2001) *Ann Clin Biochem* 38:242–251.
15. Fallarino F, Grohmann U, Vacca C, Bianchi R, Orabona C, Spreca A, Fioretti MC, Puccetti P (2002) *Cell Death Differ* 9:1069–1077.
16. Bauer TM, Jiga LP, Chuang JJ, Randazzo M, Opelz G, Terness P (2005) *Transpl Int* 18:95–100.
17. Pae HO, Oh GS, Lee BS, Rim JS, Kim YM, Chung HT (2005) *Atherosclerosis* 187:274–284.
18. Platten M, Ho PP, Youssef S, Fontoura P, Garren H, Hur EM, Gupta R, Lee LY, Kidd BA, Robinson WH, *et al.* (2005) *Science* 310:850–855.
19. Hayashi T, Beck L, Rossetto C, Gong X, Takikawa O, Takabayashi K, Broide DH, Carson DA, Raz E (2004) *J Clin Invest* 114:270–279.
20. Burke JR, Pattoli MA, Gregor KR, Brassil PJ, MacMaster JF, McIntyre KW, Yang X, Iotzova VS, Clarke W, Strnad J, *et al.* (2003) *J Biol Chem* 278:1450–1456.
21. Thome M, Martinon F, Hofmann K, Rubio V, Steiner V, Schneider P, Mattmann C, Tschopp J (1999) *J Biol Chem* 274:9962–9968.
22. Villalba M, Coudronniere N, Deckert M, Teixeiro E, Mas P, Altman A (2000) *Immunity* 12:151–160.
23. Schmitz ML, Krappmann D (2006) *Cell Death Differ* 13:834–842.
24. Harhaj EW, Sun SC (1998) *J Biol Chem* 273:25185–25190.
25. Abraham RT, Weiss A (2004) *Nat Rev Immunol* 4:301–308.
26. Casamayor A, Morrice NA, Alessi DR (1999) *Biochem J* 342:287–292.
27. Park J, Hill MM, Hess D, Brazil DP, Hofsteenge J, Hemmings BA (2001) *J Biol Chem* 276:37459–37471.
28. Wick MJ, Wick KR, Chen H, He H, Dong LQ, Quon MJ, Liu F (2002) *J Biol Chem* 277:16632–16638.
29. Wick MJ, Ramos FJ, Chen H, Quon MJ, Dong LQ, Liu F (2003) *J Biol Chem* 278:42913–42919.
30. Maiorov V, Abagyan R (1997) *Proteins* 27:410–424.
31. Kane LP, Weiss A (2003) *Immunol Rev* 192:7–20.
32. Gao X, Harris TK (2006) *Bioorg Chem* 34:200–223.
33. Schulze-Luehrmann J, Ghosh S (2006) *Immunity* 25:701–715.
34. Kelly AP, Finlay DK, Hinton HJ, Clarke RG, Fiorini E, Radtke F, Cantrell DA (2007) *EMBO J* 26:3441–3450.
35. Lee J, Mira-Arbibe L, Ulevitch RJ (2000) *J Leukoc Biol* 68:909–915.
36. Datta SK, Redecke V, Prilliman KR, Takabayashi K, Corr M, Tallant T, DiDonato J, Dziarski R, Akira S, Schoenberger SP, *et al.* (2003) *J Immunol* 170:4102–4110.
37. Broide DH, Stachnick G, Castaneda D, Nayar J, Miller M, Cho JY, Roman M, Zubeldia J, Hayashi T, Raz E (2001) *J Clin Immunol* 21:175–182.
38. Vermaelen KY, Carro-Muino I, Lambrecht BN, Pauwels RA (2001) *J Exp Med* 193:51–60.

DIRECT SUBMISSION

Sign up for PNAS Online eTocs | Get notified by email when new content goes on-line

Info for Authors | Editorial Board | About | Subscribe | Advertise | Contact | Site Map

PNAS

Proceedings of the National Academy of Sciences of the United States of America

Current Issue | Archives | Online Submission | GO | advanced search >>

Institution: Biblioteca Area Biomedica - Universita' di Roma Sign In as Member / Individual

Hayashi *et al*. 10.1073/pnas.0709261104.

Supporting Information

Files in this Data Supplement:

SI Figure 6
SI Figure 7
SI Figure 8
SI Figure 9
SI Figure 10

This Article

Abstract

Services

Email this article to a colleague
Alert me to new issues of the journal
Request Copyright Permission

Citing Articles

Citing Articles via CrossRef

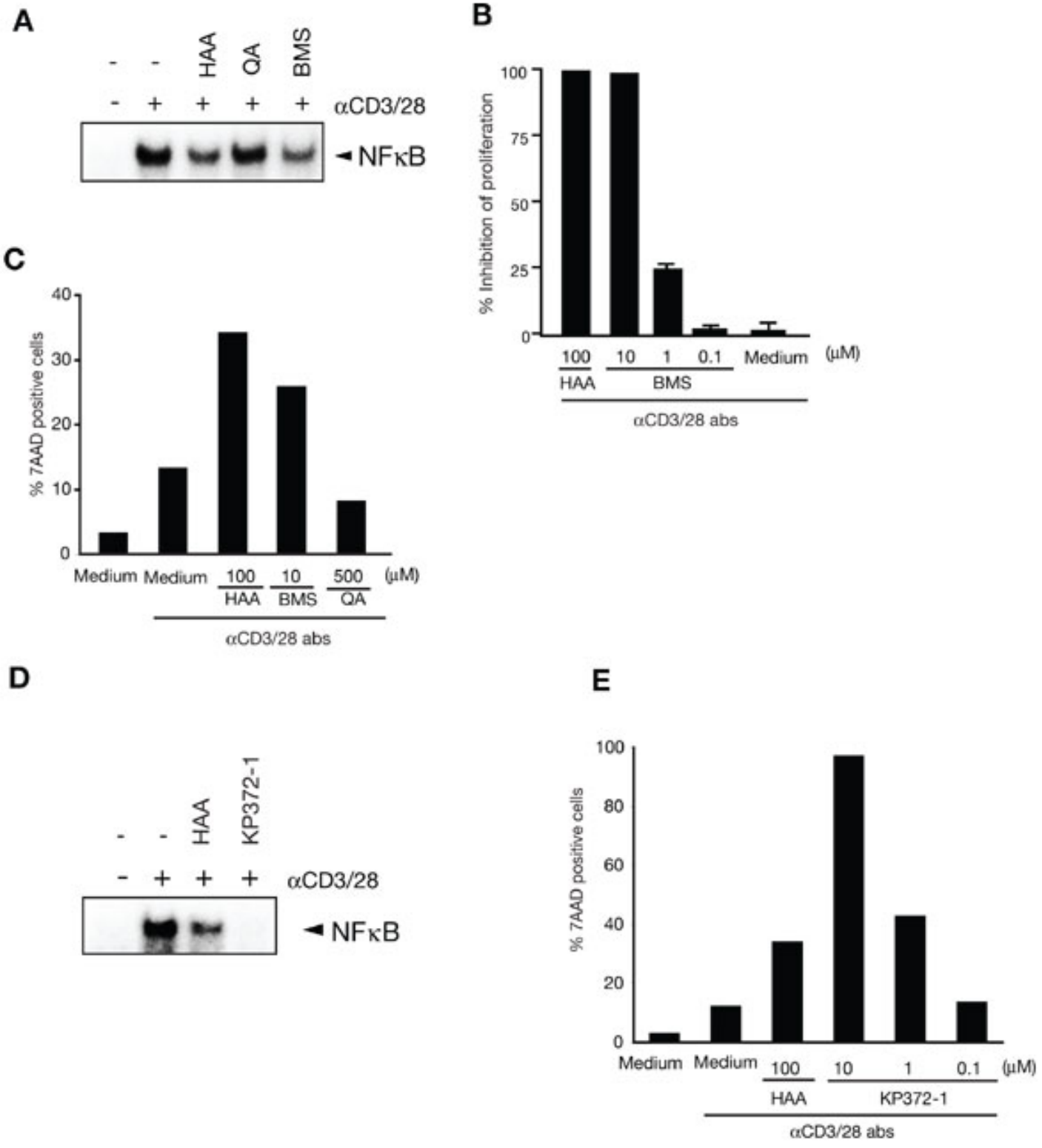

Fig. 6. Schematic illustration of the tryptophan metabolic pathway. IDO converts trp into N-formlkynurenine that is further catabolized to kynurenine, 3 hydroxykynurenine (HKYN), 3-hydroxyanthranilic acid (HAA), and then to the terminal metabolites quinolinic acid (QA), and picolinic acid (PA).

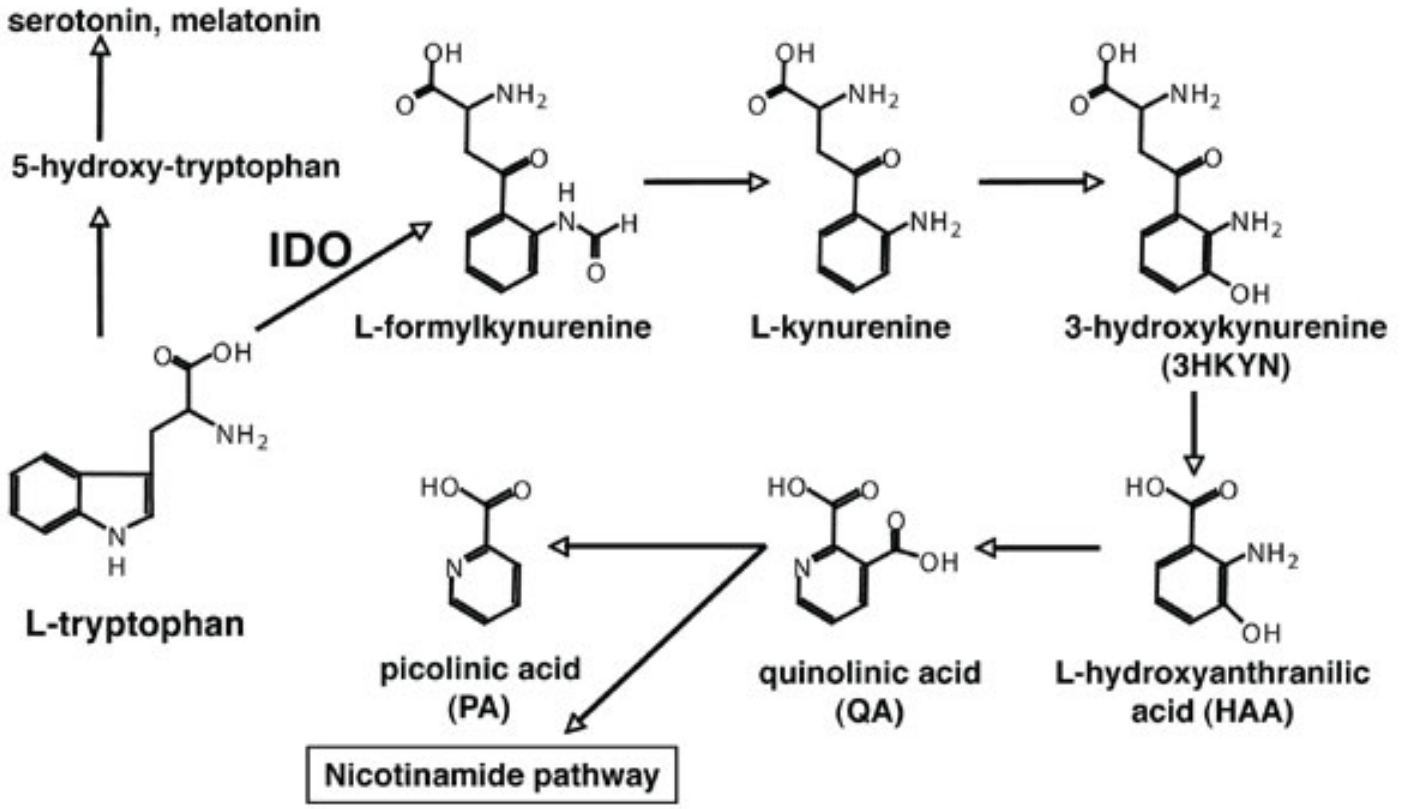

Fig. 7. HAA does not impair LPS induced dendritic cell function. (*A*) BMDC and RAW 264.7 cells were preincubated with or without HAA and stimulated with LPS. NF-kB activity was measured by EMSA. (*B*) BMDC were incubated with LPS (10 ng/ml) for 48 hrs in the presence or absence of HAA (50 or 100 μM) or QA (100 μM). The levels of IL-6, IL-12, and TNFα in the supernatants were determined by ELISA. (*C* and *D*) BMDC were incubated with LPS (10 ng/ml) in the presence or absence of HAA or QA (100 μM) for 24 hrs and the cell surface levels of CD86, CD80 or CD40 were determined by FACS. Black solid line, medium alone; dotted line, LPS (10 ng/ml); tinted with black solid line, LPS plus the trp metabolites (*C*). Changes in the expression of CD80, CD86, and CD40 were shown as the percent increase of mean fluorescent intensity compared to medium alone (*D*). (*E*) BMDC were incubated with LPS for 48 hr in the presence or absence of HAA or BMS 345541 at different concentrations. The percentage of cell death of BMDC was determined by staining with 7-AAD (FACS) and was calculated in the CD11c+ gated population.

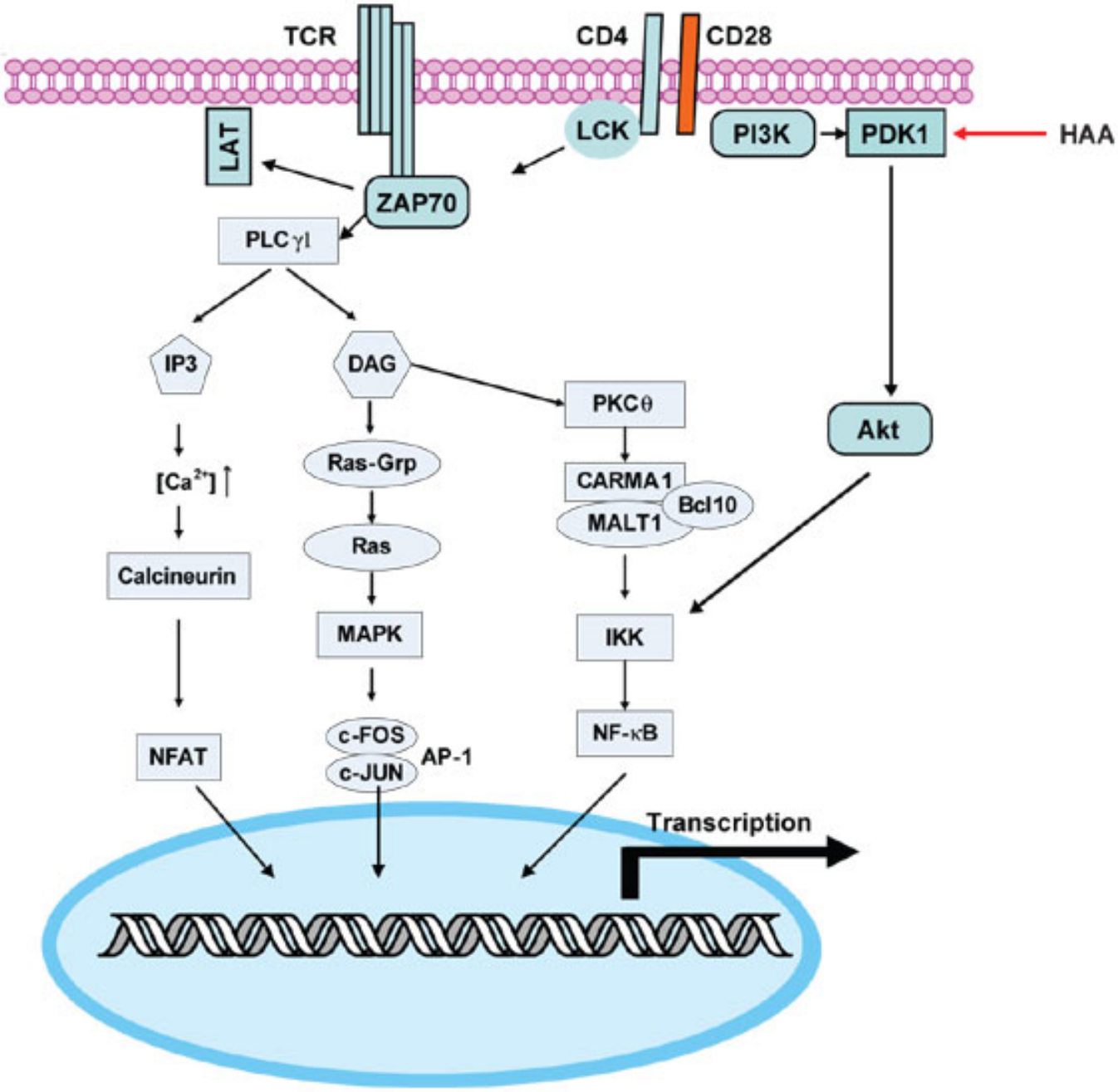

Fig. 8. Schematic illustration of TCR signaling pathways. Upon TCR stimulation, PLC-γ1 is activated generating inositol triphosphate (IP3) and diacylglycerol (DAG). IP3 induces calcium release, thus activating the NFAT pathway, and DAG phosphorilates PKCθ, thus activating the NF-kB pathway. HAA acts on PDK1, which mediates NF-kB activation via CD28 signaling.

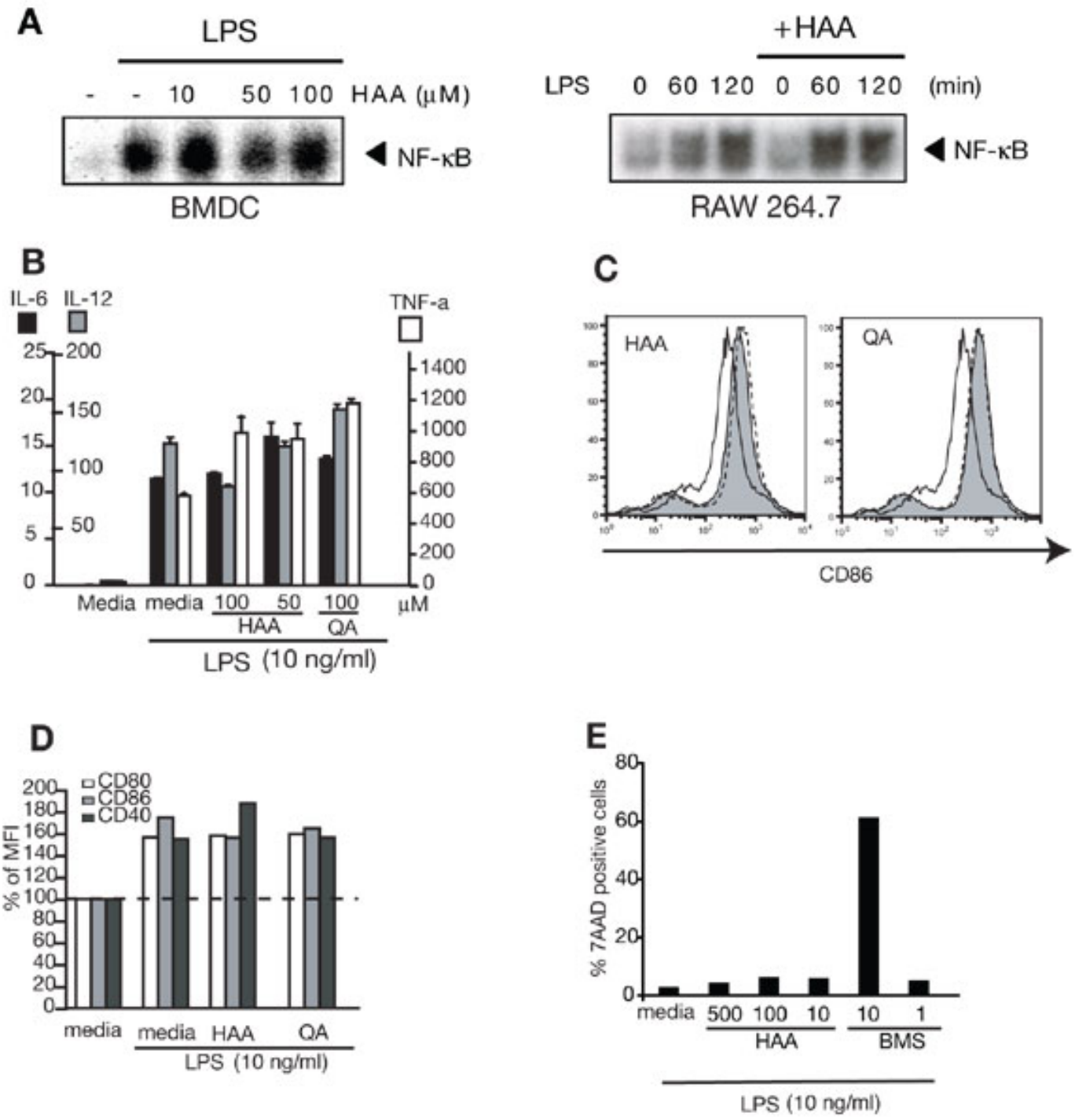

Fig. 9. HAA does not inhibit NF-kB activation induced by PKCq, Carma1, and Bcl10. HEK-293 cells were cotransfected with the indicated plasmids together with NF-kB-luciferase and β-galactosidase vectors. HAA (100 μM) was added 2 hr later. Twelve hours after transfection, cell lysates were prepared and luciferase activity was measured. Data represent NF-kB-luciferase activity normalized to β-galactosidase activity.

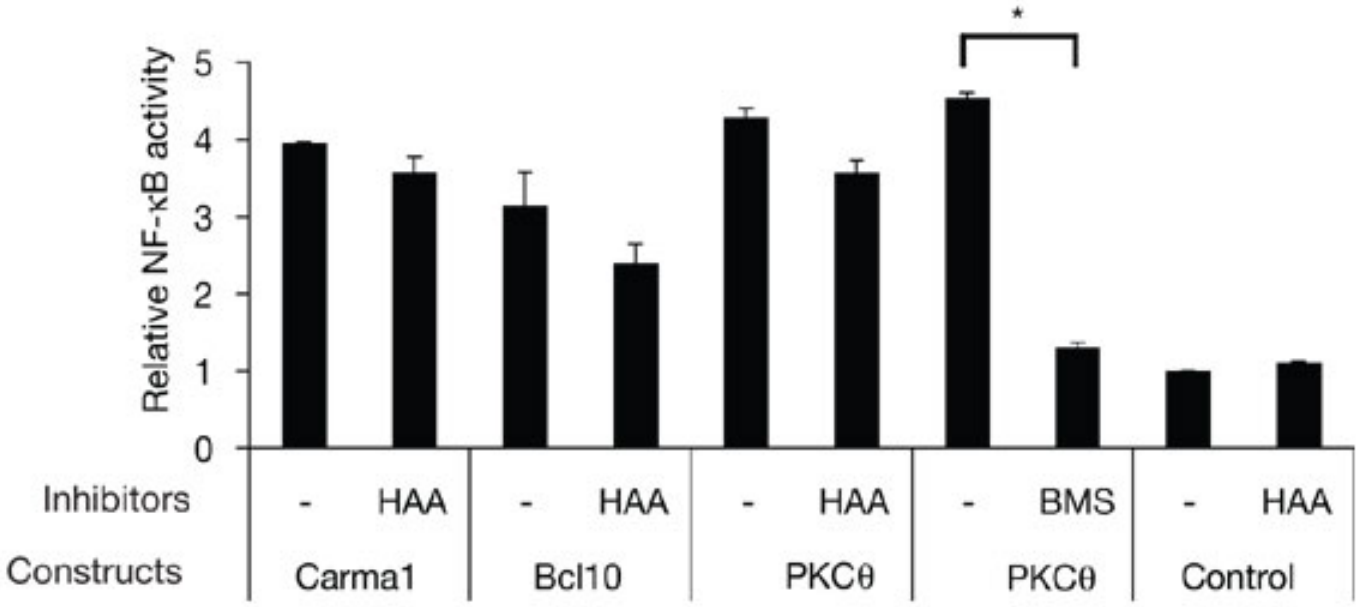

Fig. 10. BMS-345541, an NF-kB inhibitor, and KP-372-1, a PDK1 inhibitor, mimic the inhibitory effects of HAA. TgTh2 cells were preincubated with HAA, BMS-345541, or QA and then stimulated with anti CD3/CD28 mAb. (*A* and *D*) NF-kB activity was determined by EMSA. (*B*) Proliferation as determined by tritiated thymidine uptake was measured. (*C* and *E*) The percentage of cell death of tgTh2 cells was determined by staining with 7-AAD (FACS) and calculated in the CD4+/DO11.10 TCR+ gated population.

This Article

Abstract

Services

Email this article to a colleague

Alert me to new issues of the journal

Request Copyright Permission

Citing Articles

Citing Articles via CrossRef

Current Issue | Archives | Online Submission | Info for Authors | Editorial Board | About
Subscribe | Advertise | Contact | Site Map

Copyright © 2007 by the National Academy of Sciences